JOURNAL OF MATERIALS SCIENCE 29 (1994) 5407–5416

Post-deposition thermal treatments for improving the interconnection strength of a Ti–W/Au/Cu bonding system

Y. F. LUO, K. P. RAJURKAR
Nontraditional Manufacturing Research Center, University of Nebraska–Lincoln, 175 Nebraska Hall, NE 68588-0518, USA

The bonding combination of Ti–W/Au/Cu laminate strips deposited on an SiO_2/Si passivated substrate is strengthened through post-deposition age-hardening thermal treatment of the deposited metals in the amorphous state. For creating a copper layer of 10 μm thickness at the top, both electrodeposition and physical vapour deposition (evaporation) methods are applied to obtain different strip properties. Peel tests, which can simulate the strip delamination process, are conducted to evaluate the strip–substrate bonding strength. A micro-mechanics analysis indicates that weak strip stiffness is a key cause for the frequent strip–substrate separations. Consequently, the laminate composite system is heated and cooled after deposition under different treatment conditions to strengthen the strip. The specimens are heated to a temperature of 220 to 400 °C, held there for a time and cooled quickly in air or water. The strengthening effect of the amorphous metals is obvious but complicated. The improved bonding strength will decrease again if the heating temperature is lower than 200 °C or the heating time is shorter than 50 min. At room temperature, indices of performance for strip–substrate bonding strength such as average peel force, peel energy and peak peel load continuously vary within approximately 100 h, depending upon the heating treatment history. Significant improvements of up to approximately 300% have been achieved according to peel strength tests. The sticking strength becomes so high after the thermal treatment that no part of a strip can initially leave its substrate during the tests.

1. Introduction

Due to the available high processing resolution, different strip–substrate micro-interconnections based on patterning deposition technologies have ever-increasing applications in microelectronics packaging and other micro-systems. Strips are usually made very fine (width less than 50 μm) and dense to achieve high system performances. The fine and dense metallic composite strips deposited on a hard insulated substrate usually function not only as electrical conducting conduits but also as thermal conduction paths and mechanical support. Various kinds of strip failure can lead to an unreliable and low-efficiency system. Due to the large difference in terms of mechanical properties between the laminate metallic composite and the hard non-metallic substrate, the artificial interconnection is not always sufficiently strong. Frequent strip–substrate separation, like the one which occurs in the case of a Ti–W/Au/Cu strip and SiO_2/Si substrate combination, turns out to be a serious problem both during processing and in service.

A weak strip–substrate bonding can result from many factors. However, interface adhesion is often the only factor considered for studying the problem of weak strip–substrate bonding. Actually, interface adhesion deals only with the physical or chemical bond nature in an extremely thin interfacial range. Strip–substrate interconnection strength depends not only on the necessary interface adhesion, but also on the mechanical properties of the strip and substrate materials adjacent to the interface. It is understandable that the property of a thin interfacial layer cannot determine independently such overall performance as strip–substrate bonding strength. Investigations on film mechanical behaviour are necessary to understand the interconnection failure mechanism.

Thermal stress in aluminium or other strips has been investigated [1–4], as film mechanical failure is of more and more concern in the interconnection of integrated circuits. Thermal stress generated in component service time is only one of the main harmful effects. There are other destructive effects, e.g., mechanical forces at corners or edges and residual stresses in the film. Film or strip micro-mechanics under these complex effects can be complicated with various film patterns, substrate conditions and load distributions. Intrinsic stress and thermal stress other than the shear stress in the strip have also been studied analytically and numerically [3, 5]. Corresponding measurement methods of the shear stress are developed according to the substrate bending curvature in the stressed state [2, 6]. Thin and flexible strips are preferred so that intrinsic stress and thermal stress can be reduced. However, thin and flexible strips are easily separated from the hard substrates. There are two basic strip failure modes, i.e. middle breakage of strip or substrate and strip–substrate separation or delamination at strip ends. The latter occurs much more frequently than the former, since strip ends are usually subjected to peak shear stress and surrounding loads. With the normal hard substrates like silicon and AlN, rigid strips instead of flexible strips are preferred to reduce strip deformation and to enlarge the interface burden area to counteract the separation. This paper will verify the above important viewpoint experimentally and analytically. Peel tests of strip ends are conducted to examine directly the strip–substrate interconnection strength.

Annealing was the only heat treatment method used previously in metallic film processing for reducing the assumed intrinsic stress. Based on the general principle of mechanical compatibility [7], strips should be strengthened to match the hard substrate. Post-deposition heat treatments will therefore, find effective application in film processing. In the case of the Ti–W/Au/Cu/SiO_2/Si system, the strengthening effect of heat treatments can be significant. This effect turns out to be dynamic or time-dependent. Due to the original amorphous or polycrystalline state of the laminate strips after deposition, a devitrification process occurs during the heat treatment. Similar investigations [8, 9] have been reported concerning material devitrification processes of other metallic materials such as nickel and chromium. Devitrification treatments have not yet found real applications in microelectronics packaging technology concerning copper and aluminium. This paper will investigate the distinguishing effects of thermal treatment on strip–substrate bonding strength. The Ti–W/Au/Cu/SiO_2/Si system, a typical example of a flexible strip and rigid substrate, was used in all the experiments.

2. Theory for strip failure mechanisms

As developed in processing or during service, the stress distribution in a strip can vary with the actual system situation. Stress concentration, however, is always the main cause of film failure since strip failure hardly occurs in a large area simultaneously. A concentrated stress distribution is often the most serious detrimental effect. Shear stress in a strip, which is the superimposition of thermal stress and intrinsic stress, usually concentrates near the strip ends. Strip ends or corners hence become the vulnerable parts. On the other hand, strip ends are exposed to surrounding loads. In film processing, film ends or corners are subjected to various mechanical and hydraulic loads. Sometimes in film fabrication, over 50 % of the film elements may separate from the substrate after the final patterning step. The tendency to separate at strip ends is due to micro-surface deformation in a small stress-concentrated area. A thin copper layer without upper passivation cover separates more easily than an aluminium layer with a hard upper passivation. Due to the flexibility of thin copper films, partial strip separation or delamination at strip ends is the usual mode of film failure. The partial separation generated at the ends can spread quickly along the strip–substrate interface. A failure model of strip separation can be established according to static micro-mechanics as shown in Fig. 1. All loads including concentrated stress and surrounding loads at the strip end are expressed as a lifting force F so that the resisting strength against strip separation can be determined analytically.

The thin strip can be considered as a wide beam which is subject to a lifting force at its end. The wide beam curvature is given by the second-order differential equation

$$\frac{d^2v}{dx^2} = -(1-\nu_f)\frac{\int_x^L r(t)(t-x)dt}{E_f I_f} \qquad (1)$$

where v is the beam displacement in the y direction, $r(x)$ is the normal stress distribution in the strip–substrate interface, E_f, I_f and ν_f are the strip's E-modulus, moment of inertia and Poisson's ratio, respectively, and L is defined as the burden length. When $x > L$, $r(x)$ and the bending moment in the strip can be omitted. For the moment to be in equilibrium,

$$\int_0^\infty r(x)x\,dx = 0 \qquad (2)$$

Thus the distribution function is obviously cyclic and degenerative in nature. Let

$$r(x) = r(0)e^{-bx}\cos(bx) \qquad (3)$$

where parameter b is concerned with materials properties and the size of the bonding structure.

On the substrate side, we have a generalized two-dimensional Hooke's law:

$$\varepsilon_{yy} = \frac{1-\nu_s}{E_s}\sigma_{yy} \qquad (4)$$

where ε_{yy} is substrate strain in the y direction, σ_{yy} is substrate stress in the y direction, and E_s and ν_s are substrate E-modulus and Poisson's ratio, respectively.

At the interface

$$\varepsilon_{yy} = v/h \qquad (5)$$

$$\sigma_{yy} = r(x)/w \qquad (6)$$

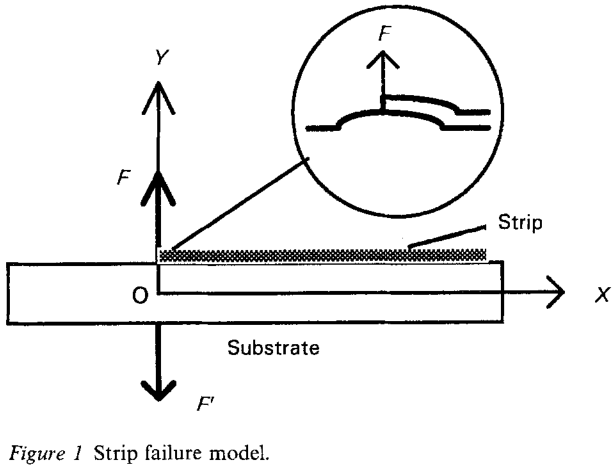

Figure 1 Strip failure model.

where w is strip width. Thus, substituting Equations 5 and 6 into Equation 4,

$$v = \frac{(1 - \nu_s)h}{E_s w} r(x) = \frac{(1 - \nu_s)h}{E_s w} r(0) e^{-bx} \cos(bx) \quad (7)$$

Substituting Equation 7 into Equation 1

$$b = \frac{1}{2^{1/2}} \left(\frac{w E_s (1 - \nu_f)}{h E_f I_f (1 - \nu_s)} \right)^{1/4} \quad (8)$$

$$F = -\int_0^{\infty} r(x) dx = -\frac{r(0)}{2b} \quad (9)$$

Considering Equation 3, one can determine the burden length L as follows. $r(x)$ varies cyclically and decreases along the interface. Only the first half-cycle contributes to the increase in lifting force at the strip end:

$$L = \pi/2b \quad (10)$$

A large F corresponds with large E_f and I_f, and small E_s and I_s. According to Equation 3, the decline of $r(x)$ along the direction X depends upon L. With a larger value of L, i.e. a relatively more rigid strip and softer substrate, the bonding combination can be subject to a greater separating force F. A large L indicate a long burden length of the interface under the pull load, and a small decreasing rate of the interface stress distribution $r(x)$ along direction X as well. It is indicated that a combination of substrate and strip with similar material properties is preferred to achieve strong bonding. This is the fundamental conclusion on which an important principle of mechanical compatibility is based.

Even with an adhesion layer as base, a thin copper strip does not stick to a hard silicon substrate well enough, and separation occurs frequently even at the strip processing stage. The above micro-mechanics analysis reveals that the low anti-bending rigidity of a strip which is loaded on its edge or corner results in severe micro-stress concentration and reduces the interface burden length. In other words, the loaded interface area becomes constricted when the strip bends too flexibly. Strips can be separated from the substrate under only a small destructive load. Hence, separation occurs even with perfect interface adhesion and under a low stress level because only a very small part of the interface is required to resist the separation. Stress concentration, in addition to constriction of the resisting area, results in interconnection failure. It is necessary to increase the strip's strength so that strips become mechanically compatible with the hard substrate. Therefore, heat treatments can find effective application in modifying the microstructure of the metallic composite strip. Through such heat treatment the strip rigidity can be increased just after strip deposition.

3. Experimental procedure

In order to obtain a strong strip–substrate bonding, high strip–substrate adhesion and low intrinsic stress are important, but they are not the only requirements in patterning, deposition and subsequent treatment processes. These two obvious factors always attract more attention than another important factor, i.e. the material properties of the bonded elements. This investigation will focus attention upon the latter factor. Post-deposition thermal treatments are conducted to strengthen the thin strips. The effects of deposition processes on strip density are also taken into consideration when different deposition processes are applied.

As for the composite laminates Ti–W/Au/Cu, each layer has a different function such as adhesion layer, diffusion barrier, conducting line, sometimes a wettable soldering base and so on. As far as strip–substrate interconnection strength is concerned, surface preparation becomes important for perfect interface adhesion. Good interface adhesion is always a prerequisite for the interconnection although it cannot guarantee strong bonding independently. Procedures of surface preparation and the deposition process are described below to obtain a good interface adhesion. Due to the advantages of plasma cleaning and the high energy of the depositing atoms, as well as of the atom bombardment, sputtering is used instead of evaporation for bottom layer deposition, so that the adhesion between the bottom sputtered layer and the substrate can be significantly improved.

After solvent cleaning, the passivated surface of the silicon wafer is cleaned with an O_2 plasma for 5 min. Sputter-cleaning is conducted *in situ* just prior to the Ti–W(N) sputtering deposition. High-frequency sputtering is applied for creating a 10 nm thick 5 % Ti–95 %W layer adhering to the passivated silicon substrate. After the Ti–W layer is sputtered on the cleaned wafer surface in nitrogen gas, a gold layer, also 10 nm thick, is sputtered on the Ti–W layer as a further deposition base. The sputtering parameters are carefully chosen so that the intrinsic stress in the deposited layer is minimized. Later, another quick deposition process is required to grow the upper bulk copper layer on the sputtered base.

The metallized wafer surface is cleaned again through an O_2 plasma. The surface is then patterned with a positive photoresist layer 20 μm thick. With a current density of 1 A dm^{-2}, a copper layer of thickness 10 μm is electroplated on the patterned surface. The electrodeposition process lasts for 50 min. Another tin layer is also electroplated for patterning protection. Thereafter, the photoresist with the upper tin layer can be stripped off in the acetone solvent. The same O_2 plasma cleaning is conducted just after the pattern strip-off. Extra gold and Ti–W parts are etched in an erosive medium for 130 and 10 s, respectively.

Physical vapour deposition (PVD) evaporation was substituted for the electroplating process. It is noted that the material properties of evaporated and electroplated copper layers are different. Significant improvements in peel strength were achieved due to this substitution because the evaporated copper layer is denser than the electroplated layer. After the final step of strip construction, further processing such as cleaning and cutting should be carefully conducted because the soft strips can easily be separated from the substrate in the processing. Further measures for improving interface adhesion, such as conducting strict cleaning and changing the deposition conditions, were conducted in our efforts to strengthen the weak interconnection. These measures for increasing the strip–substrate bonding strength turned out to be in vain.

Pull tests were carried out for confirming interface adhesion after careful processing. The adhesion test (pulling) values always showed a satisfactory result. The pull load limit usually reached $20\ \mathrm{N\,mm^{-2}}$ or higher. The actual adhesion strength may be much higher than the measured value because interface separation under pull load is controlled by surface deformation and partial fractures process.

The film rigidity can be improved through various measures. Heat treatment, well known as an effective method for modifying the mechanical properties of crystalline metals, is applied here for modifying the mechanical properties of the laminate's non-crystalline composite. Instead of matching an equilibrium state for stress relief, the composite is changed from one non-equilibrium state to another non-equilibrium state through the heat treatment so that the E-moduli of the film materials can be increased. The heat treatment can harden the strips without reducing the interface adhesion after specimen cooling. Thus, the strips can match the hard substrate mechanically in the stressed state. Specimens are usually heated for 10 min to 2 h and to a temperature of 200 to 400 °C. Thereafter, the heated specimens are cooled quickly in air or water. It is noted that some time-dependent effect occurs both during heating and after cooling.

4. Results and discussion

4.1. Strip peel tests

Experimentally, a pertinent test method should be used to examine the strip-substrate interconnection strength. Pull tests and peel tests are two direct measuring methods. In a pull test, a solid part connected with the upper surface of the thin film is required for applying a pull load. Consequently, surface strain is limited by the solid holder and the test results can be affected by the holder. As recorded in the pull tests, the peak pull load or separating limit force provides a complex index containing information from both the interface adhesion and the material strength of the strip–substrate couple, since not only the interface bond but also materials in the neighborhood of the interface are mechanically loaded during the pull test. Interface adhesion cannot be evaluated simply according to the peak pull load: a low peak pull load may result from low material strength instead of low interface adhesion. However, a high peak pull load always promises good interface adhesion. After conducting the proper depositions mentioned in the previous section, the pull strength limit measured in pull tests always reached a satisfactory value ($10–30\ \mathrm{N\,mm^{-2}}$). This indicates good adhesion and high material strength of the Ti–W/Au/Cu and SiO_2/Si combination system. In spite of the good interface adhesion, a bonding strength problem still exists in processing; it appears that frequent strip separations cannot be further reduced simply through improving the interface adhesion.

Strips were found to be extremely vulnerable to peel load at the ends or corners. With a small peel load of only several millinewtons the strips can easily separate from the substrate. Because the peel test just simulates the separation process without the effect of the upper specimen holder, a peel test instead of a pull test was chosen for evaluating the strip–substrate bonding strength. Usually, strip separation always began at the strip end and the small and partial separation expanded quickly along the interface. Strip ends were observed to be the weakest parts. The ends receive external fluid and mechanical forces in processing and during service. On the other hand shear stress, which is the thermal stress plus intrinsic stress in the interfacial region, will be concentrated very close to the strip ends. A peel test does not change the surface strain mode like a pull test. Simulating outside and inside separation effects, the peel test applies a load at the strip end and reveals exact information about the strip failure process. Thus, peel tests are a more pertinent examination for strip–substrate bonding strength than the popular pull test.

It is noted that direct mechanical tests are unusual for microstructures. There is no test standard for such a thin film of only 20 μm thick. In our investigation a standard strip width of 2 mm was taken for all experiments so that a comparative peel load value could be obtained. This standard width is an enlarged value for the convenience of the peel tests because the small peel load can increased with a wide strip. With the enlarged strip, the bonding strength problems can easily be found. The real strip width will be reduced according to the strip function requirements. The peel test system consists of an Instron 4502 automated test machine with data acquisition and processing function. A peeling device without any sliding mechanism is used to prevent additional disturbances. A light and long copper wire, 0.8 m long, connects one end of the examined strip, 10–30 mm in length, with the machine upper terminal, where a force transducer is mounted. According to the overall test results, a small inclination of such a long wire has little influence on the measured values of peel load. As shown in Fig. 2, a theoretical curve for the peel load can be developed according to the separation mechanics. A peak load

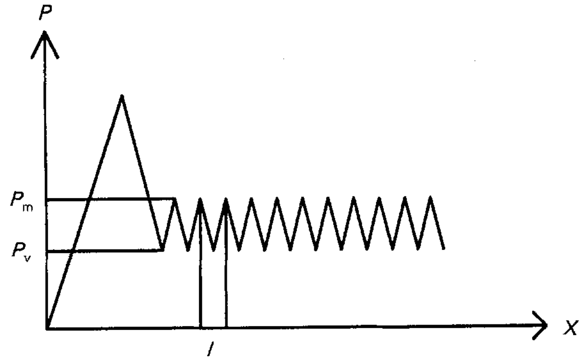

Figure 2 Theoretical curve of peel load versus distance.

appears at the beginning of the force–distance curve, as a bending moment is required to bend the strip initially to its vertical position. Measured curves are identical except for some variation and noise. For evaluating strip–substrate bonding strength, the following five indices of performance are available from the test curve:

1. Average peel load P_a (N):

$$P_a = \frac{\int_0^L P(x)\mathrm{d}x}{L} \tag{11}$$

where L is the total measured length (mm), x the peeling distance (mm) and $P(x)$ the measured peel load at point x. P_a shows the average peel load recorded by the data acquisition system. This value, however depends on the strip width.

2. Peel strength J ($\mathrm{N\,mm^{-1}}$):

$$J = \frac{\int_0^L P(x)\mathrm{d}x}{wL} \tag{12}$$

where w is the strip width (2 mm). J is independent of strip width. It can properly represent the strip anti-separation strength.

3. Peak peel load P_m (N). There are some peaks on the test curve in addition to the initial peak load. The peak loads are cyclically distributed on the test curve, which indicate the maximum peel force required to separate the strip.

4. Valley peel load P_v (N). After a peak load, a valley load usually follows. The release of stored elastic energy causes a quick separation and hence a valley peel load.

5. Cycle length l (mm). The cycle length of the peel load vibration indicates the burden length achieved on the interface under peel load.

In a peel test the examined strip leaves its substrate section by section as it proceeds to peel intermittently. The speed of the test pulling device is set to a low value of 0.5–2.5 $\mathrm{mm\,min^{-1}}$ so that the test can be regarded as a static process. A peel test of the thin films serves well as a comprehensive and direct measurement for interconnection strength. The peel load necessary for separating the strip depends on the interface adhesion strength, interface burden length and shear stress in the interfacial region. The interface burden length is the main consideration of this investigation. Different heat treatments were applied to improve strip rigidity. Thus, a stiff strip with a long burden length can be achieved through post-deposition thermal treatment.

After peel tests, the separated surfaces are further examined through an optical microscope and scanning electron microscope (SEM). Fig. 3 shows four distinguishing surface types which reveal different interface fracture modes:

1. Mode A: Fig. 3a shows a quite smooth separated surface. However, under the scanning electron microscope, microfracture pits on the smooth surface are still discernible. This smooth separation mode reveals interface adhesion failure accompanied by substrate surface fracture very close to the interface. In this mode, the strip bending curvature can be extremely small with little burden area, or the strip can be very rigid with little bending.

2. Mode B: in Fig. 3b, equally distributed deep fracture grooves can be discerned on the separated surface of the substrate. This groove separation mode reveals a pure substrate breakage with no adhesion failure. Under peel load, significant stress and strain occur in a small substrate surface layer near the interface because of strip bending and burden area constriction. The strip burden length increases with groove width.

3. Mode C: Fig. 3c, obtained with an optical microscope, shows another type of separated surface mode with pure and flat substrate breakage. Fig. 3d shows an SEM picture of the same separated surface, which turns out to be flat with few very fine broken grooves in the silicon. A flat separation mode usually indicates high interconnection strength.

4. Mode D: Fig. 3e is another optical microscopy picture of a smooth separated surface with long fractures equally distributed on the surface. This long fracture mode indicates a small strip bending curvature and high peak peel load. Sudden separation with high peak peel load occurs in this mode.

It is noted that abundant surface topographies occur only after post-deposition heat treatments. Without heat treatment the separated surfaces are always smooth, and no fractures or grooves can be observed under a microscope. Some characteristics of the peel test curve are correlated with different surface separation modes. The peel test reveals a lot of information about bonding strength and the separation process itself. Special heat treatments can change the system properties tremendously.

4.2. Heat treatments

Table I provides peel test results of original specimens without any heat treatment. The peel strength of an evaporated strip is approximately 90% higher than the peel strength of an electroplated strip, as the evaporated strip is much denser and thus more rigid than the electroplated one. Only a smooth surface mode (mode A) can be observed on the separated surfaces of original specimens. A deposited copper strip with a base layer, irrespective of its type, electroplated or evaporated, possesses mechanical properties typical of common glassy metals such as high ductility and yield strength. Thus, the deposited laminate strips are not in configurational equilibrium, but are relaxing slowly by a homogeneous process towards an "ideal" metastable amorphous state or polycrystalline state. As mentioned above, the purpose of heat treatments is to increase strip rigidity. In the treatment experiments, the heating temperature is set lower than the crystallization temperature of the metallic elements concerned. After heat treatment, interlayer diffusion and intermetallic compounds cannot be clearly observed under the optical microscope and SEM. Considerable peel strength variation after heat treat-

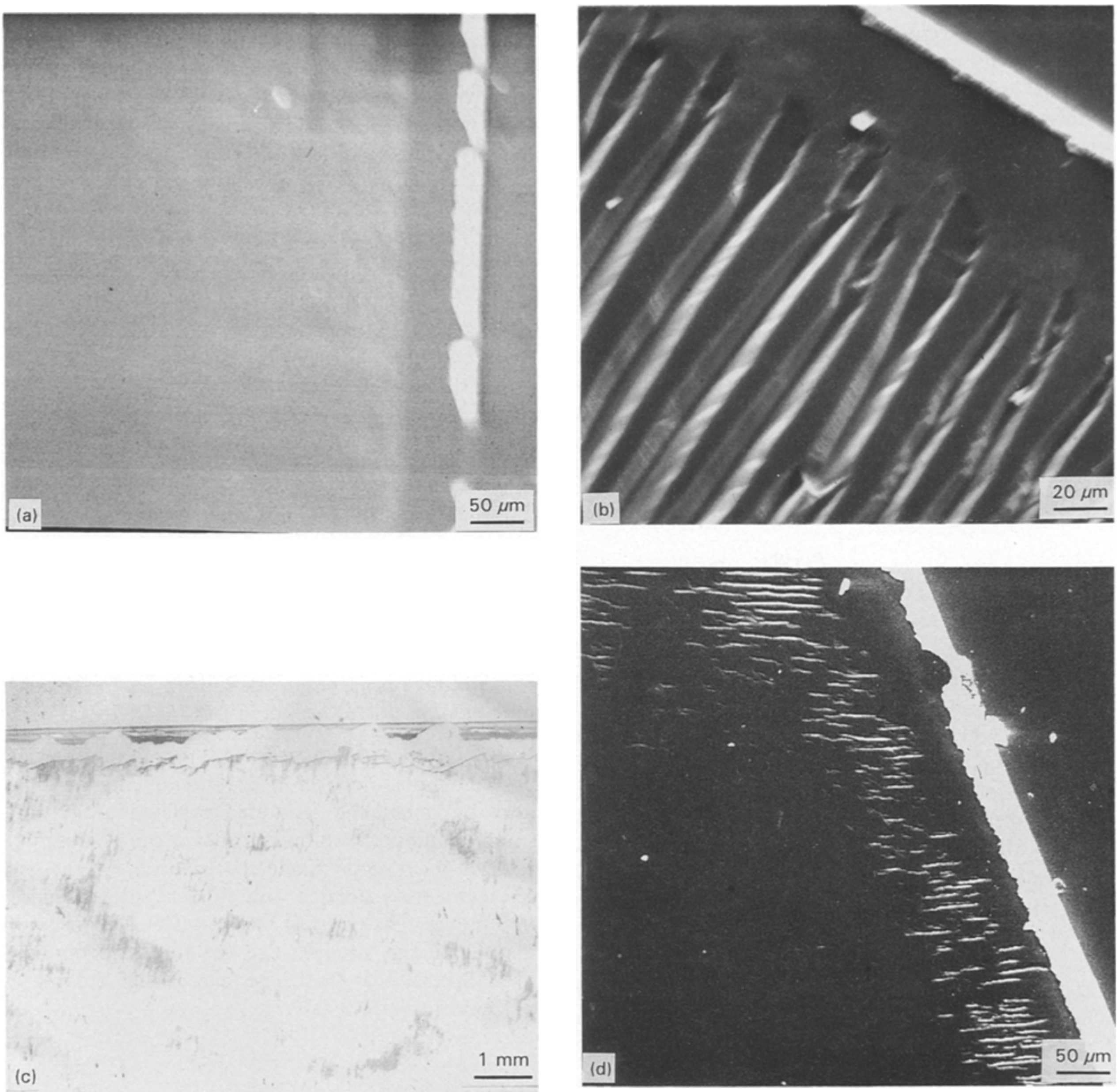

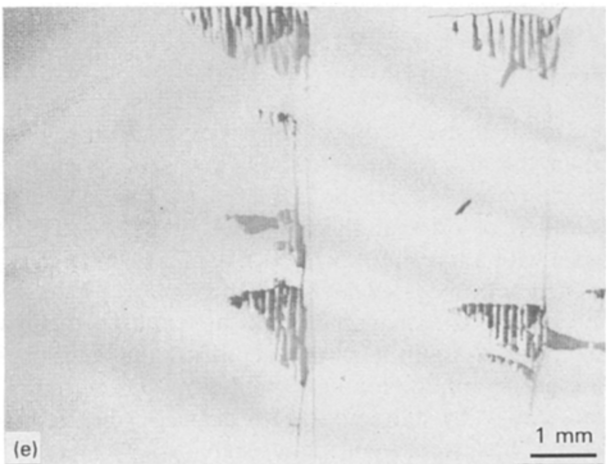

Figure 3 (a) Smooth separation mode (SEM), (b) groove separation mode (SEM), (c) flat silicon breakage (optical microscopy), (d) flat breakage mode (SEM), (e) long fracture mode (optical microscopy).

TABLE I Original peel strength of specimens without thermal treatment

Deposition type	Peel force (mN)	Peel strength ($mN\,mm^{-1}$)	Surface mode
Electroplating	8.5	4.3	Smooth
Evaporation	15.8	7.9	Smooth

ment demonstrates a special dynamics of materials change in the deposited films after heat treatment.

According to long-term peel tests, the material properties continuously change at room temperature after thermal treatment. Fig. 4 shows peel test results obtained for different durations of cooling. An electroplated specimen was heated to a temperature of 250 °C and held there for 1.2 h. The heated specimen was then cooled quickly by quenching in water. The first peel test was conducted 10 min after cooling began. The second and third peeling tests were performed 26 and 106 h after the cooling began. Curves 1, 2 and 3 in Fig. 4a show test results of the first, second and third peeling test, respectively. The group of optical microscopy pictures in Fig. 4b–d demonstrate the evolution

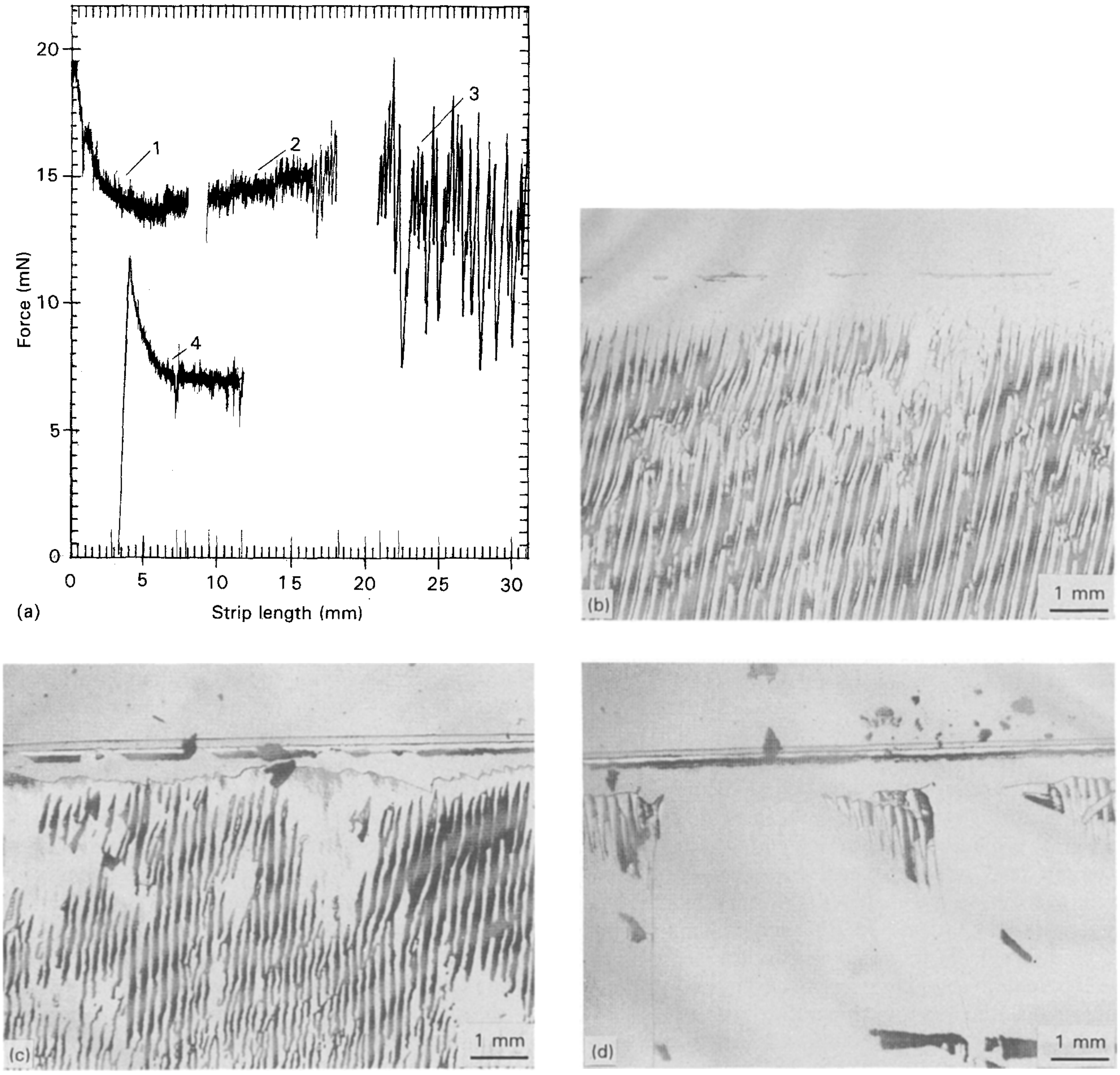

Figure 4 (a) Long-term peel tests: (1) first, (2) second and (3) third test; (4) original specimen. (b–d) Optical microscopy of surface after first, second and third test, respectively.

of surface separation modes corresponding to the first, second and third test, respectively. Compared with the peel strength of the original specimen as shown by curve 4 in Fig. 4a, considerable improvement in peel strength can be achieved through thermal treatment since the strip rigidity can be increased in the treatment. As indicated by the long-term peel tests, the mechanical properties of a strip vary continuously for several days after the cooling began. The peak load rises and the cycle length extends due to some age-hardening effects. Correspondingly, the surface separation mode is also changing after the cooling begins. It is certain that some new phases or foreign particles precipitate after the quick cooling.

Fig. 5 shows another group of curves recorded in a long-term peel test. In this experiment, an electroplated specimen was heated to a temperature of 220 °C and the specimen heating lasted only for 15 min. The heated specimen was cooled quickly in air. The first peel test, conducted 10 min after specimen cooling, was recorded as curve 1 in Fig. 5. Curves 2 and 3 show peel test results recorded at 42 and 67 h, respectively, after specimen cooling. As shown in Fig. 5, the initially improved peel strength decreases dramatically in subsequent days due to some negative post-treatment material change. The first peel test opened up a separated surface with rupture grooves (mode B). The second and third peel test, however revealed smoothly separated surfaces (mode A). The surface separation mode varied with strip–substrate bonding strength and peel test time after the treatment. If the heating time is short or the heating temperature is low, a strip strengthened in post-deposition thermal treatment can completely relax several days after the treatment. Approximately speaking, a heating temperature higher than 200 °C and a heating time longer than 1 h are required for a lasting high bonding strength to be achieved in the thermal treatments. Material

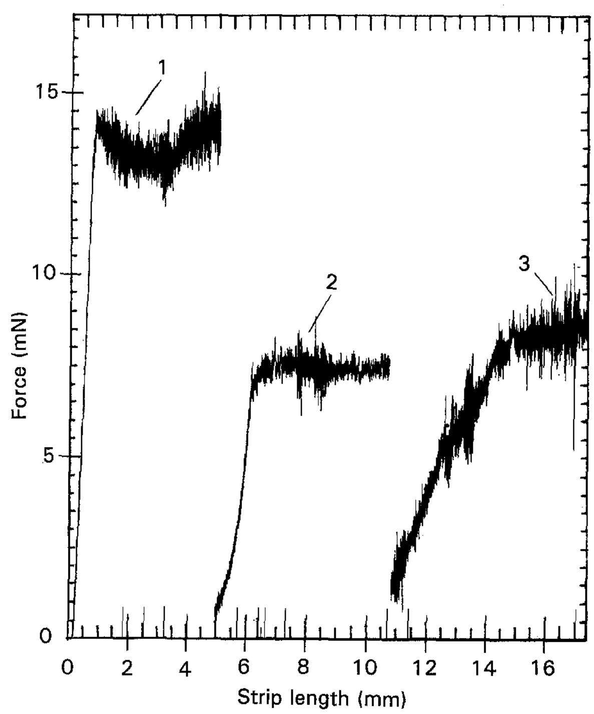

Figure 5 Peel strength fall after thermal treatment: (1) 10 min, (2) 42 h and (3) 67 h. After specimen cooling.

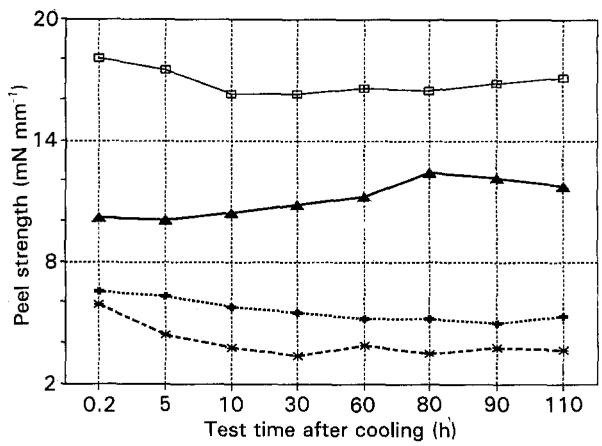

Figure 6 Peel strength evolution of heat-treated specimens with electroplated Cu film: (×) 200 °C, 1.5 h; (+) 240 °C, 1.5 h; (▲) 280 °C, 1.5 h; (□) 320 °C, 2 h.

microstructural change of the glassy laminates needs to take some time, and requires a high temperature so that the positive treatment effect can be maintained.

Fig. 6 provides the experimental results of peel strength tests when the heat treatment parameters were changed to meet different treatment conditions. Fig. 6 shows that with a top electroplated copper layer, a significant improvement in peel strength can be expected through heat treatment. The peel strength increases as the heating temperature rises in the temperature region of 200 to 400 °C. All heated specimens were cooled in air immediately. The heating time was 2 h for all these specimen treatments. Compared with the original peel strength of 4 $mN\,mm^{-1}$ for electroplated specimens, thermal treatments with the heating temperature higher than 200 °C can increase the peel strength by more than 30 % and up to 300 %. As shown in Fig. 6, an initially improved peel strength can later be reduced a little, especially with a low heating temperature of about 200–240 °C. However, the improved peel strength can be maintained if the heating temperature is higher than 240 °C or so. As shown in the figure, the long-term peel strength can be improved by 300 % through thermal treatment. The surface separation mode of specimens treated at a heating temperature of 200 °C changed from the groove mode (mode B) to the smooth mode (mode A) while the peel strength dropped significantly several days after the treatment. When treated at a heating temperature of 240 °C, specimens always showed a separated surface mode with surface grooves (mode B). The surface separation mode of specimens treated thermally at 280 °C was always a flat substrate breakage mode (mode C). However, a smooth separated surface with long fractures (mode D) can be observed on the specimen surface after peeling when electroplated specimens are treated thermally at 320 °C.

Fig. 7 shows similar experimental results concerning PVD evaporated specimens instead of electroplated specimens. Here also the heated specimens were cooled in air immediately. The original peel strength (approximately 7.5 $mN\,mm^{-1}$) of evaporated specimens is much higher than for the electroplated ones (approximately 4 $mN\,mm^{-1}$). As shown in Fig. 7, the peel strength of evaporated specimens can also be improved significantly through thermal treatment. A peel strength of almost 40 $mN\,mm^{-1}$ has been reached, as for the evaporated specimens. The surface separation mode for PVD evaporated specimens was always the smooth separation mode (mode A) both with and without thermal treatment.

Although further improvement in peel strength through thermal treatment is possible by increasing the heating temperature, the peel test will become difficult because with a peel strength higher than 40 $mN\,mm^{-1}$ no part of strip end can be initially separated from the substrate. Further improvement through post-deposition heat treatment can be expected according to the test results obtained. Even longer-lasting experiments showed that the improved bonding strength would never be reduced if it remained strong several days after thermal treatment. It was noted that the pull strength measured in a pulling test instead of a peeling test showed no difference between the original specimens without any treatment and the thermally treated ones.

The peak peel load is another criterion for the bonding strength. Fig. 8 shows the evolution of the peak peel load of an electroplated specimen after thermal treatment. Long-term peel tests reveal that the peak peel load keeps building up after the treatment. Specimens were heated to a temperature of 200 to 320 °C for a sufficiently long time of about 2 h. The measured peak peel load rises significantly as a certain age-hardening effect proceeds at room temperature (20 °C). Fig. 8 shows that peak peel loads up to 60 mN can be reached. Fig. 9 shows similar experimental results concerning the peak peel loads of PVD evaporated specimens. A similar peak load increase after the treatment can be observed as for evaporated specimens, when the heating temperature is high enough. It

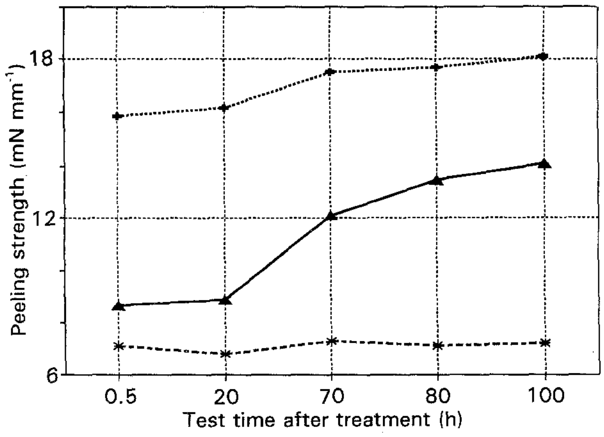

Figure 7 Peel strength evolution of heat-treated specimens with evaporated Cu film: (×) 200 °C, 2 h; (▲) 240 °C, 2 h (+) 280 °C, 2 h.

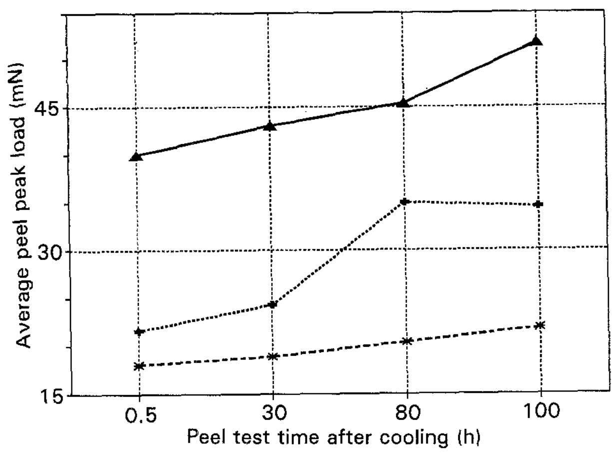

Figure 8 Average peak load evolution of heat-treated electroplated specimens: (×) 240 °C, 2 h; (+) 280 °C, 2 h; (▲)320 °C, 2 h.

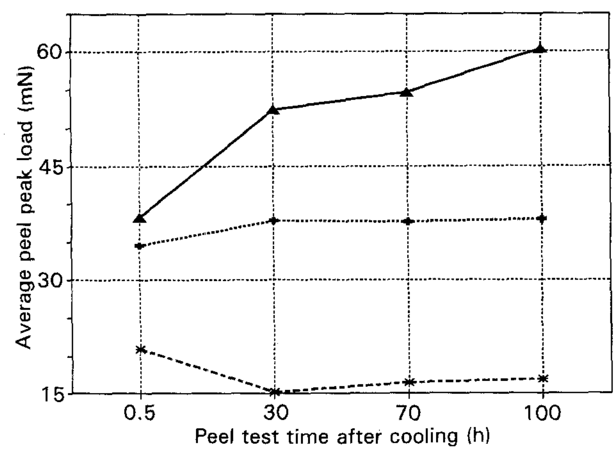

Figure 9 Average peak load evolution of heat-treated evaporated specimens: (×) 200 °C, 2 h; (+) 240 °C, 2 h; (▲) 280 °C, 2 h.

is noted that the cycle length of peel test curves of evaporated specimens is longer than that of electroplated ones. Obviously, a certain precipitation process occurs at room temperature after specimen cooling in addition to devitrification of the deposited metals during specimen heating.

5. Summary

In accordance with a general strip failure model based on planar elasticity theory, low strip anti-bending rigidity turns out to be a main reason for the frequent strip separation from a hard substrate. Various destructive effects on the strip–substrate interconnection, e.g. shear stress and surrounding loads, are manifested as a lifting force at the strip end. Strips with high *E*-modulus and cross-section area moment of inertia can bear a large lifting force at the strip end. In post-deposition thermal treatments, the material system of Ti–W/Au/Cu strips deposited on an SiO_2/Si substrate was heat-treated at a temperature of 200 to 400 °C and cooled quickly in air or water. After the thermal treatment, the ductile strip becomes much harder so that it can match its hard substrate mechanically much better than the original strip. The bonding strength can be measured through peel tests which properly simulate the separation process.

Without any thermal treatment, strips with an upper evaporated copper layer adhere more strongly to the substrate than those with an electroplated copper layer. About 90 % improvement can be reached by the substitution of copper electroplating by copper PVD evaporation. This phenomenon provides evidence that the denser and more rigid evaporated strips possess a higher strip–substrate bonding strength.

A lasting improvement in peel strength of more than 300 % can be achieved when an electroplated specimen is heated to 320 °C and held there for 2 h. A lasting improvement in peel strength of more than 200 % can be achieved when an evaporated specimen is heated at a temperature of 280 °C for 2 h. In both cases, heated specimens are cooled quickly in air. During subsequent days after the post-deposition treatment, the peak peel load will rise significantly. Further improvement through thermal treatment with higher heating temperature is still possible, but peel tests become difficult or impossible. Long-term peel tests and examinations of the surface separation mode demonstrate complex material dynamics caused by the strip post-deposition heat treatment.

Besides the devitrification process during thermal treatment, some precipitation occurs at room temperature in composite laminates with an upper copper layer. Because three layers of material are involved in the thermal treatment, the effects of the treatment on each individual layer have not been separated. No significant interlayer diffusion could be observed in experiments where the specimens were treated under the stated conditions. Comprehensive investigations are expected in the future. The micro-mechanics and material dynamics revealed in this paper are of great significance for the production and reliability of micro-components with metallic composite films.

Acknowledgements

The encouragement and advice provided by Professor H. Reichl and Dr G. Chmiel of the Technical University, Berlin, are gratefully acknowledged. The authors would also like to thank Mr. Sunder Mohan for his assistance in the preparation of the manuscript.

References

1. D. S. GARDNER and P. A. FLINN, *IEEE Trans. Electron. Dev.* **35** (1988) 2160.
2. P. A. FLINN, D. S. GARDNER and W. D. NIX, *ibid.* **ED-34** (1987) 689.
3. I. SAUTER and W. D. NIX, *IEEE Trans. Compon. Hybr. & Mfg Technol.*, **15**, (1992) 594.
4. B. J. ALECK, *J. Appl. Mech.*, **16** (1949) 118.
5. M. F. DOERNER and W. D. NIX, *CRC Crit. Rev. Solid State Mater. Sci.* **14** (1988) 225.
6. A. SEGMULLER, J. ANGILELO and S. J. LaPLACA, *J. Appl. Phys.*, **51**, 6224.
7. Y. F. LUO and K. P. RAJURKAR, in Proceedings of ASME Winter Syposium on Manufacturing Aspects in Electronic Packaging, 1993, in press.
8. RUNG-YWAN TSAI and SHINN-TYAN WU, *J. Electrochem. Soc.* **136**, 1341.
9. M. YAMAMOTO, K. SHIRAI and N. WATANABE, *ibid.* **138**, 2082.
10. W. J. TOMLISOM, R. V. WINKLE and L. A. BLACKMORE, *IEEE Trans. Hybr., Comp. & Mfg Technol.* **13**, (1990) 587.
11. W. CHEN, *ibid.* **13** (1990) 553.
12. W. DALLY and W. F. RILEY, "Experimental Stress Analysis" (McGraw-Hill, New York, 1978).
13. D. V. DUNFORD and P. G. PATRIDGE, *J. Mater. Sci.* **27** (1992) 5769.
14. K. I. MIZUISHI and T. MORI, *IEEE Trans. Hybr. Comp. & Mfg Technol.* **11** (1988) 481.
15. M. N. NGUYEG, *ibid.* **13** (1990) 478.
16. R. R. TUMMALA and E. J. RYMASZEWSKI, "Microelectronic Packaging Handbook" (Van Nostrand-Reinhold, New York, 1988).
17. K. G. HIENEN, W. H. SCHROEN *et al.*, in Proceedings of 38th Electronic Components Conference, Los Angeles, CA, 1988, p. 672.
18. E. ZAKEL, J. KLOESER, J. SIMON and F. BECHTOLD, in "Micro System Technologies 92", Proceedings of 3rd International Conference on Micro Electro, Opto, Mechanics Systems and Components, Berlin, 1992, (vde-Verlag, Berlin) p. 89.
19. S. LACAZE and L. ANQUEZ, *J. Mater. Sci.* **27** (1992) 5982.
20. W. H. KNAUSENBERGER and M. R. PINNEL, *Mater. Res. Soc. Symp. Proc.* **72** (1987) 255.
21. F. R. BUNSH AH, "Handbook of Deposition Technologies for Film and Coatings" (Noyes, Park Ridge, NJ, 1994).
22. N. MOLDOVAN, L. CSEPREGI, A. KLUMPP and W. LANG, in "Micro System Technologies 92", Proceedings of 3rd International Conference on Micro Electro, Opto, Mechanic Systems and Components, Berlin, 1992, (vde-Verlag, Berlin) p. 105.

Received 29 July 1993
and accepted 19 January 1994